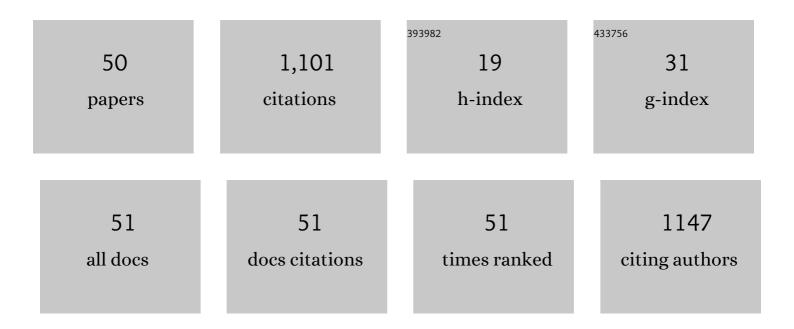
Kaushik Biswas

List of Publications by Year in descending order

Source: https://exaly.com/author-pdf/5684482/publications.pdf Version: 2024-02-01



#	Article	IF	CITATIONS
1	Concentration-dependent luminescence of Tb3+ ions in high calcium aluminosilicate glasses. Journal of Luminescence, 2009, 129, 1347-1355.	1.5	123
2	Luminescence Properties of Dual Valence Eu Doped Nano-crystalline BaF2 Embedded Glass-ceramics and Observation of Eu2+ → Eu3+ Energy Transfer. Journal of Fluorescence, 2012, 22, 745-752.	1.3	73
3	Concentration quenched luminescence and energy transfer analysis of Nd3+ ion doped Ba-Al-metaphosphate laser glasses. Applied Physics B: Lasers and Optics, 2010, 101, 235-244.	1.1	59
4	Enhanced Blue Emission from Transparent Oxyfluoride Glass–Ceramics Containing Pr ³⁺ :BaF ₂ Nanocrystals. Journal of the American Ceramic Society, 2010, 93, 1010-1017.	1.9	59
5	Influence of bismuth on structural, elastic and spectroscopic properties of Nd3+ doped Zinc–Boro-Bismuthate glasses. Journal of Luminescence, 2014, 149, 163-169.	1.5	52
6	Sensitized red luminescence from Bi3+ co-doped Eu3+: ZnO–B2O3 glasses. Physica B: Condensed Matter, 2009, 404, 3525-3529.	1.3	48
7	Crystallization kinetics of amorphous Fe67Co9.5Nd3Dy0.5B20. Journal of Alloys and Compounds, 2005, 397, 104-109.	2.8	44
8	Enhanced 2μm broad-band emission and NIR to visible frequency up-conversion from Ho3+/Yb3+ co-doped Bi2O3–GeO2–ZnO glasses. Spectrochimica Acta - Part A: Molecular and Biomolecular Spectroscopy, 2013, 112, 301-308.	2.0	40
9	Effect of boron oxide addition on structural, thermal, in vitro bioactivity and antibacterial properties of bioactive glasses in the base S53P4 composition. Journal of Non-Crystalline Solids, 2018, 498, 204-215.	1.5	40
10	Broadband Er^3+ emission in highly nonlinear Bismuth modified Zinc-Borate glasses. Optical Materials Express, 2011, 1, 344.	1.6	37
11	Efficient non-resonant energy transfer in Nd^3+-Yb^3+ codoped Ba-Al-metaphosphate glasses. Journal of the Optical Society of America B: Optical Physics, 2010, 27, 2750.	0.9	35
12	Effect of melt convection on the secondary dendritic arm spacing in peritectic Nd–Fe–B alloy. Journal of Alloys and Compounds, 2009, 480, 295-298.	2.8	26
13	Synthesis and Structural Probing of <scp><scp>Eu³⁺</scp></scp> Doped <scp><scp>BaYF₅</scp></scp> Nanoâ€Crystals in Transparent Oxyfluoride Glassâ€Ceramics. International Journal of Applied Glass Science, 2012, 3, 154-162.	1.0	26
14	Crystallization kinetics analysis of BaF2 and BaGdF5 nanocrystals precipitated from oxyfluoride glass systems: A comparative study. Thermochimica Acta, 2015, 610, 1-9.	1.2	25
15	Preparation of alumino-phosphate glass by microwave radiation. Journal of Materials Research, 2013, 28, 1955-1961.	1.2	24
16	Near-infrared frequency down-conversion and cross-relaxation in Eu2+/Eu3+–Yb3+ doped transparent oxyfluoride glass and glass–ceramics. Journal of Alloys and Compounds, 2014, 608, 266-271.	2.8	24
17	Enhanced 1.8μm emission in Yb3+/Tm3+ co-doped tellurite glass: Effects of Yb3+↔Tm3+ energy transfer and back transfer. Journal of Quantitative Spectroscopy and Radiative Transfer, 2014, 147, 112-120.	1.1	22
18	Role of Yb3+ ions on enhanced ~2.9 μm emission from Ho3+ ions in low phonon oxide glass system. Scientific Reports, 2016, 6, 29203.	1.6	22

#	Article	IF	CITATIONS
19	In vitro bioactivity and antibacterial properties of bismuth oxide modified bioactive glasses. Journal of Materials Research, 2018, 33, 178-190.	1.2	22

Formation and spectral probing of transparent oxyfluoride glass-ceramics containing (Eu2+,) Tj ETQq0 0 0 rgBT /Overlock 10 $\frac{11}{20}$ 50 702 T

21	Time Resolved Fluorescence and Energy Transfer Analysis of Nd3+–Yb3+–Er3+ Triply-Doped Ba–Al-Metaphosphate Glasses for an Eye Safe Emission (1.54Âμm). Journal of Fluorescence, 2010, 20, 425-434.	1.3	17
22	Midâ€IR transparent TeO ₂ â€TiO ₂ â€La ₂ O ₃ glass and its crystallization behavior for photonic applications. Journal of the American Ceramic Society, 2018, 101, 3900-3916.	1.9	16
23	On the fragility of Cu47Ti33Zr11Ni8Si1metallic glass. Journal Physics D: Applied Physics, 2006, 39, 2600-2608.	1.3	15
24	Insights into Er 3+ ↔Yb 3+ energy transfer dynamics upon infrared ~1550 nm excitation in a low phonon fluoro-tellurite glass system. Journal of Luminescence, 2017, 187, 441-448.	1.5	15
25	Glass-forming ability and fragility parameter of amorphous Fe67Co9.5Nd3Dy0.5B20. Journal of Applied Physics, 2006, 100, 023501.	1.1	14
26	Realization of warm white light from Ce-Eu-Tb doped zinc fluoroboro silicate glass for lighting applications. Journal of Alloys and Compounds, 2018, 747, 242-249.	2.8	14
27	Eu3+doped ferroelectric BaBi2Ta2O9 based glass-ceramic nanocomposites: Crystallization kinetics and energy storage properties. Journal of Alloys and Compounds, 2018, 740, 237-249.	2.8	14
28	Structure and Stability of High CaO- and P2O5-Containing Silicate and Borosilicate Bioactive Glasses. Journal of Physical Chemistry B, 2019, 123, 7558-7569.	1.2	14
29	Nonisothermal crystallization kinetics and microstructure evolution of calcium lanthanum metaborate glass. Journal of Thermal Analysis and Calorimetry, 2010, 101, 143-151.	2.0	13
30	Elucidating the effect of CaF2 on structure, biocompatibility and antibacterial properties of S53P4 glass. Journal of Alloys and Compounds, 2020, 831, 154704.	2.8	13
31	Enhanced nearâ€infrared to green upconversion from Er 3+ â€doped oxyfluoride glass and glass ceramics containing BaGdF 5 nanocrystals. International Journal of Applied Glass Science, 2017, 8, 204-215.	1.0	12
32	Structural elucidation of NASICON (Na ₃ Al ₂ P ₃ O ₁₂) based glass electrolyte materials: effective influence of boron and gallium. RSC Advances, 2018, 8, 14422-14433.	1.7	12
33	Enhanced luminescence at 2.88 and 2.04 μm from Ho3+/Yb3+ codoped low phonon energy TeO2–TiO2–La2O3 glass. AlP Advances, 2019, 9, .	0.6	11
34	Tailoring the microstructure and mechanical properties of Ti–Al alloy using a novel electromagnetic stirring method. Scripta Materialia, 2006, 55, 1143-1146.	2.6	10
35	Bandwidth enhancement of MIR emission in Yb3+/Er3+/Dy3+triply doped fluoro-tellurite glass. Laser Physics Letters, 2017, 14, 035804.	0.6	10
36	Fabrication of bulk amorphous Fe67Co9.5Nd3Dy0.5B20 alloy by hot extrusion of ribbon and study of the magnetic properties. Journal of Materials Science, 2006, 41, 3445-3450.	1.7	9

Kaushik Biswas

#	Article	IF	CITATIONS
37	Al2O3 influence on structural, elastic, thermal properties of Yb3+ doped Ba–La-tellurite glass: Evidence of reduction in self-radiation trapping at 1μm emission. Spectrochimica Acta - Part A: Molecular and Biomolecular Spectroscopy, 2014, 133, 318-325.	2.0	9
38	Experimental evidence for quantum cutting co-operative energy transfer process in Pr3+/Yb3+ ions co-doped fluorotellurite glass: dispute over energy transfer mechanism. Physical Chemistry Chemical Physics, 2016, 18, 33115-33125.	1.3	8
39	Influence of Ho ₂ O ₃ on Optimizing Nanostructured Ln ₂ Te ₆ O ₁₅ <i>Anti</i> ã€Glass Phases to Attain Transparent TeO ₂ â€Based Glassâ€Ceramics for Midâ€IR Photonic Applications. Advanced Engineering Materials. 2020. 22. 1901357.	1.6	8
40	Effect of TiO2 on thermal, structural and third-order nonlinear optical properties of Ca–La–B–O glass system. Journal of Alloys and Compounds, 2010, 489, 493-498.	2.8	7
41	Complete suppression of metastable phase and significant enhancement of magnetic properties of B-rich PrFeB nanocomposites prepared by devitrifying amorphous ribbons. Journal of Magnetism and Magnetic Materials, 2007, 308, 24-27.	1.0	6
42	Role of iodine in broadening the optical window of As Sb S I chalcogenide glass system. Journal of Non-Crystalline Solids, 2017, 470, 47-52.	1.5	6
43	Structural modification associated with Al ₂ O ₃ addition in oxyfluoride glasses: Thermal and mechanical properties. Journal of the American Ceramic Society, 2017, 100, 5490-5501.	1.9	5
44	Controlling melt convection—an innovation potential for concerted microstructure evolution of Nd-Fe-B alloys. Materials Science & Engineering A: Structural Materials: Properties, Microstructure and Processing, 2005, 413-414, 302-305.	2.6	4
45	Frequency upconversion mechanism in Ho3+/Yb3+-codoped TeO2–TiO2–La2O3 glasses. Applied Physics B: Lasers and Optics, 2019, 125, 1.	1.1	4
46	Correlation between Raman spectroscopy and mechanical properties of As-Sb-S-I chalcogenide glasses. Journal of Non-Crystalline Solids, 2019, 507, 56-65.	1.5	4
47	Structure and magnetic properties in Ag-stabilized ferromagnetic sensor of CrO2 nanoparticles. Materials Science & Engineering A: Structural Materials: Properties, Microstructure and Processing, 2008, 498, 125-128.	2.6	3
48	Broad NIR emission near c - Si band gap from Bi-doped Ba–Al metaphosphate glasses as promising solar spectral converter. Journal of Materials Science, 2015, 50, 5450-5457.	1.7	3
49	Factors governing the sinterability, In vitro dissolution, apatite formation and antibacterial properties in B2O3 incorporated S53P4 based glass powders. Ceramics International, 2022, 48, 4512-4525.	2.3	3
50	Influence of melt convection on microstructure evolution of Nd-Fe-B alloys using a forced crucible rotation technique. Physica Status Solidi C: Current Topics in Solid State Physics, 2006, 3, 3277-3280.	0.8	1